Design and Control of a MEMS Microengine Fabricated from Asymmetrical Polysilicon Surface Micromachined Electrothermal Microactuators

Edward S. Kolesar, Alfred J. Jayachandran, William E. Odom and Matthew D. Ruff

***Abstract*—This research is focused on the design and experimental characterization of two types of MEMS asymmetrical electrothermal microactuators. Both microactuator design variants use resistive (Joule) heating to generate thermal expansion and movement. Deflection and force measurements of both microactuators as a function of applied electrical power are presented. Also described is the practical integration of the electrothermal microactuators in a monolithic microengine that has been operated to control the position of a mechanical shuttle.**

***Index Terms*—Microelectromechanical System (MEMS), Electrothermal microactuator, Cantilever, Microengine**

I. Introduction

The seamless integration of conventional microelectronics with three-dimensional, microdynamic, mechanical components can readily be accomplished using microelectromechanical systems (MEMS) technology. Numerous electrically driven microactuators have been investigated for positioning individual elements in microelectromechanical systems (MEMS). The most common modes of actuation are electrostatic, magnetostatic, piezoelectric and thermal expansion [1]. Unfortunately, the forces produced by electrostatic and magnetostatic actuators tend to be small, and to achieve large displacements, it is necessary to either apply a large voltage or operate the devices in a resonant mode. On the other hand, piezoelectric and thermal expansion actuators can be configured to produce large forces and large displacements. Unfortunately, piezoelectric materials are not routinely supported in the fabrication processes offered by commercial MEMS foundries. As a result, these limitations have focused attention on thermally-actuated devices for generating large forces and displacements [2].

Manuscript received November 1, 2002. This work was supported in part by the Lockheed Martin Corporation, Tactical Aircraft Systems Division, Fort Worth, TX, grant N-549-SOW-7009357; the Presby Corporation, Dallas, TX, grant 70410-43502-23356, Texas Christian University, Office of Research and Sponsored Projects, grant TCU/RCAF 11950-43502-60205; and the National Science Foundation, grant CTS-9601283.

E.S. Kolesar, A.J. Jayachandran, W.E. Odom and M.D. Ruff are with Texas Christian University, Department of Engineering, Fort Worth, TX 76129 USA (E.S. Kolesar is the corresponding author. Telephone 817-257-6226; fax: 817-257-7704; e-mail: e.kolesar@tcu.edu).

This research focuses on improving the design and experimental performance of the MEMS electrothermal microactuator [3]–[8]. As depicted in Fig. 1, the conventional MEMS polysilicon electrothermal microactuator uses resistive (Joule) heating to generate thermal expansion and movement [8]. When current is passed through the actuator from anchor-to-anchor, the larger current density in the narrower “hot” arm causes it to heat and expand along its length more than the “cold” arm. Since both arms are joined at their free (released) ends, the difference in length of the two arms causes the microactuator tip to move in an arc-like pattern about the flexure element incorporated at the anchor end of the “cold” arm. Removing the current from the device allows it to return to its equilibrium state.

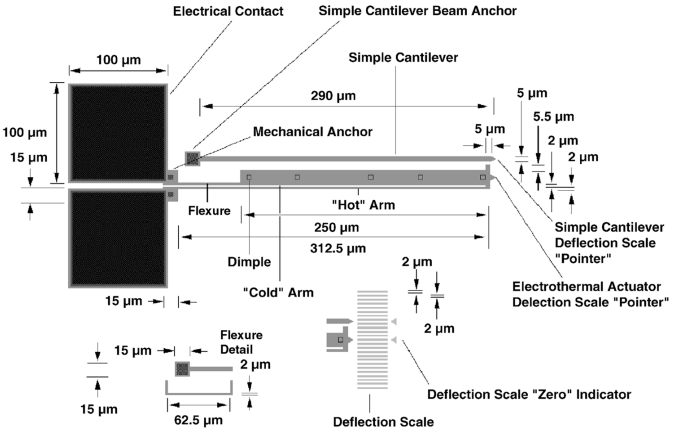

Fig. 1. Conventional single–“hot” arm polysilicon electrothermal actuator design with an adjacent simple cantilever used to measure deflection force. The inset depicts a magnified view of the thermal beam’s tip (“pointer” feature) and scale used to measure deflection.

The design of the flexure used in an electrothermal microactuator is an important functional element [7]. Ideally, the flexure element should be as narrow as possible. Narrower flexures allow more of the force generated by the thermal expansion of the “hot” arm to cause movement at the tip of the microactuator. In the conventional electrothermal microactuator depicted in Fig. 1, electrical current passes through the flexure. If the flexure were to be narrower than the “hot” arm, the temperature of the flexure element would be greater than the “hot” arm, and it could be destroyed by excessive heat. Additionally, the flexure element needs to be sufficiently long

so that it can be elastically deflected by the thermally-induced length expansion of the "hot" arm. However, if the flexure is too long, movement of the microactuator's tip will be significantly reduced. That is, long flexures will also expand in length when electrical current is applied, thus countering the intended rotational movement. The flexure and "cold" arm contribute to the microactuator's overall electrical resistance because they complete the electrical circuit for current passing through the "hot" arm. Furthermore, the power dissipated in the flexure and "cold" arm does not contribute to the desired movement of the actuator. Only the power dissipated in the "hot" arm directly translates into the intended movement of the actuator. The flexure and "cold" arm feature accounts for approximately 25 percent of the net electrical resistance of the conventional electrothermal microactuator illustrated in Fig. 1. The new electrothermal microactuator design depicted in Fig. 2 eliminates the parasitic electrical resistance of the "cold" arm by incorporating an additional "hot" arm. The second "hot" arm improves electrical efficiency by providing an active return current path. Additionally, the rotating "cold" arm can now have a narrower flexure element compared to the flexure in a conventional device (Fig. 1) because it no longer needs to conduct an electrical current. The narrower flexure also improves the microactuator's mechanical efficiency [7]. As shown in Fig. 2, an improvement in the design of the double-"hot" arm electrothermal actuator has been achieved by making the outer "hot" arm slightly longer than the inner "hot" arm. This feature prevents the arms from contacting each other.

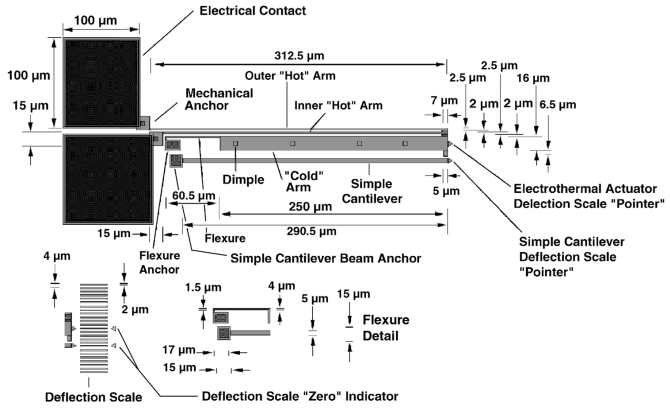

Fig. 2. Improved double–"hot" arm polysilicon electrothermal microactuator design with an adjacent simple cantilever used to measure deflection force.

II. Design and Fabrication

The design of the two electrothermal microactuators was accomplished with the L-Edit® CAD software program [9], and the devices were fabricated using the MUMPs foundry service [10]. The electrothermal actuator arms were fabricated from the 2 µm thick, stress-free, electrically-conductive, *poly 1* releasable structural layer (Figs. 1 and 2). The authors have previously reported that a practical "hot" arm width is 2 µm, and that a 62 µm long flexure yielded excellent performance [8], so these parameters were not varied in this investigation. However, the width of the flexure was reduced in the double–"hot" arm microactuator variant, and the lengths of the electrothermal microactuators were systematically varied by changing the length of the "cold" arm. Table 1 summarizes the critical dimensions of the single– and double–"hot" arm electrothermal microactuators that were investigated.

Adjacent to the pair of mechanical anchors for the "hot" and "cold" arms in the single–"hot" arm microactuator, and the two "hot" arms in the double–"hot" arm device, are pairs of adjoining electrical contact pads composed of a stacked layer of *poly 1*, *poly 2*, and gold. The physical size of the contact pads (100 µm square) facilitates either making repetitive mechanical probe contacts (or implementing permanent wire bonds). The electrothermal actuator tip deflection scale and the equilibrium rest position triangular index marker (Figs. 1 and 2) were rendered using the *poly 0* structural layer. To minimize stiction problems that are commonly associated with the wet chemical sacrificial glass release etch process, the MUMPs carbon dioxide (CO_2) critical-point drying scheme was utilized [10].

To experimentally measure the force that can be generated at the tip of an activated electrothermal microactuator, a long and narrow simple cantilever was positioned parallel to the "cold" arm in each design (Figs. 1 and 2). The end of the 5 µm wide simple cantilevers closest to the electrical contact pads was anchored to the silicon nitride substrate. Two dimple structures (each 1 µm square) were uniformly spaced along the simple cantilevers to minimize frictional losses from contact with the silicon nitride substrate during in-plane translation. The deflection marker positioned at the other end of the simple cantilever was incorporated along with a *poly 0* deflection scale to measure the simple cantilever's in-plane translation when contacted by an activated electrothermal microactuator. The physical gap between the deflectable tips of the simple cantilever and the electrothermal microactuator's "cold" arm was 2 µm.

III. Experimental

The tip deflection characteristics of the two electrothermal microactuator design variants were experimentally measured using a Karl Suss microprobe station (model PM 5; 2000 x magnification), a pair of Karl Suss RF microprobes (model PH 150), and a Keithley electrometer/programmable DC power supply (model 617). To implement these measurements, the simple cantilever (Figs. 1 and 2) used to accomplish the tip force measurement was carefully removed with a microprobe. The tip deflection magnitudes for the set of single–"hot" arm and double–"hot" arm electrothermal microactuators described in Table 1 were measured as a function of the externally applied DC voltage and current. While accomplishing these measurements, it was observed that when the "cold" arm length (Table 1) was greater than or equal to 300 µm, the motion of the microactuator was very irregular and erratic; otherwise the motion of the shorter devices was very smooth and highly reproducible. A subsequent high-magnification microscopy investigation revealed that when the "cold" arm length was greater than or equal to 300 µm, the released end of the actuator was being deflected by gravity, and it made physical contact with the substrate. The plot illustrated in Fig. 3 cap-

tures the measured tip deflection characteristics of the single–"hot" arm and double–"hot" arm electrothermal microactuators for "cold" arm lengths (Table 1) equal to 250 µm versus the activation electrical power (activation voltage x activation current). For both electrothermal microactuator design variants, this "cold" arm length manifested the largest tip deflection magnitude. The two plot symbols represent the experimentally measured data, and the line represents the non-linear least-squares curve fit.

Several authors have modeled the deflection characteristics of the electrothermal actuator, and they have reported that the activation power (W) can be related to tip displacement (d) by an m^{th}-power relationship (that is, $d = k \times W^m$, where k is a constant of proportionality) [1]—[8]. The smooth curves depicted in Fig. 3 represent the Levenburg-Marquardt non-linear least-squares curve fit calculated results for the two electrothermal microactuator design variants.

Figs. 1 and 2 depict the geometry and position of the adjacent simple cantilever that was used to measure the lateral force imparted on it by the tip of an activated electrothermal microactuator. Cochin and Cadwallender [11] have modeled the incremental side-to-side deflection (d) of a simple cantilever due to the application of an in-plane force applied to its tip (F_{tip}) as:

$$F_{tip} = \frac{E h}{4} \left(\frac{b}{l}\right)^3 d$$

where losses due to friction have been ignored, and E = Young's modulus of elasticity (average value of 160 Gpa for the MUMPs polysilicon [10]), h = the cantilever's width (e.g., Figs. 1 and 2; 10 µm), b = the cantilever's thickness (2 µm for the MUMPs *poly 1* [10]), and l = the cantilever's suspended length (e.g., Figs. 1 and 2; 290.5 µm).

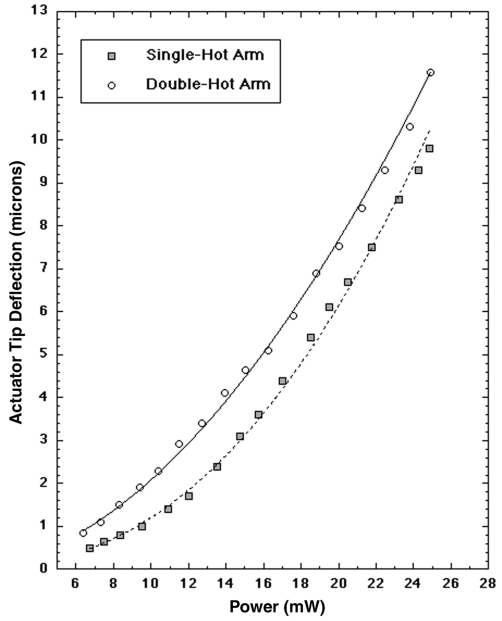

Fig. 3. Plot of tip deflection (d) versus activation electrical power (mW) for the single–"hot" arm and double–"hot" arm electrothermal microactuator design variants whose "cold" arm lengths are 250 µm. The plot symbols depict the averaged experimentally measured results for five different electrothermal actuators. The smooth curve corresponds to the Levenburg-Marquardt non-linear least-squares curve fit for an equation of the form: d (µm) = k (µm/mW) x [W (mW)]^m ; (k = 0.005, m = 2.344 and Corr. Coef. = 0.962 for the single–"hot" arm actuator, and k = 0.028, m = 1.875 and Corr. Coef. = 0.947 for the double–"hot" arm actuator).

For each of the single–"hot" arm and double–"hot" arm electrothermal microactuator design variants, five devices for each of the six different "cold" arm lengths were experimentally characterized to establish tip generated force. Once again, it was observed that when the "cold" arm length (Table 1) was greater than or equal to 300 µm, the motion of the two microactuator designs was very irregular and erratic; otherwise the motion of the shorter devices was very smooth and highly reproducible.

The Karl Suss microprobe station was used to measure the tip deflection of the simple cantilever, and the Keithley electrometer/programmable DC power supply was used to apply the activation power. Table 2 summarizes the average values of the tip forces generated by each of the functional electrothermal microactuators.

The resonance frequency the single– and double–"hot" arm electrothermal microactuators was measured to be 69.73 kHz and 54.62 kHz, respectively [8].

As a result of the performance of the single– and double–"hot" arm electrothermal microactuators, the practical implementation of a MEMS microengine was accomplished. Fig. 4 depicts a microengine that incorporates a shuttle whose bi-directional linear motion can be controlled by activating two independent sets of orthogonal mechanical elements. One of the mechanical elements is called the pawl, and when it is activated by the set of three parallel single–"hot" arm electrothermal actuators, it contacts the translator element. Activation of the set of eight double–"hot" arm electrothermal actuators causes the translator element to move, correspondingly causing

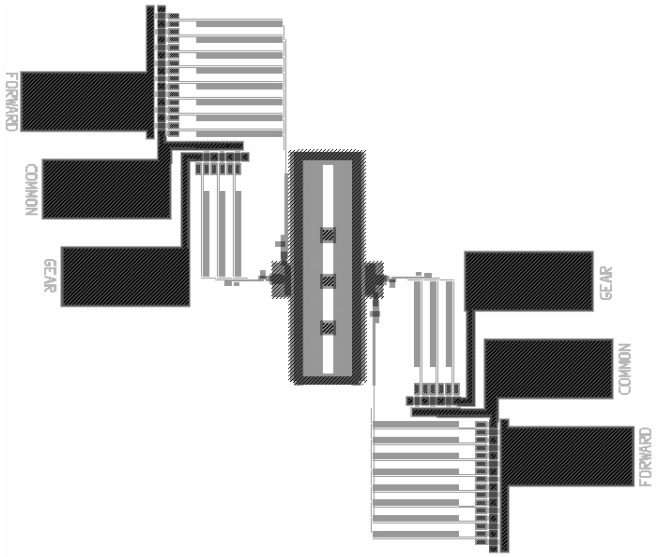

Fig. 4. CAD layout of the electrothermal microengine and mechanical shuttle. The linear translator that contacts the shuttle is connected with a mechanical yoke to the array of eight parallel double–"hot" arm electrothermal actuators. When the array of three parallel single–"hot" arm electrothermal elements is activated, the pawl contacts the translator. When the geared translator element contacts the mechanical shuttle, linear motion is achieved when the array of ten double–"hot" arms is activated. The electrothermal arrays on the left side of the shuttle control its motion in the downward direction, and the set on the right side control its motion in the upward direction.

Table 1. Dimensions of the Critical Components in the Single– and Double– "Hot" Arm Electrothermal Microactuators. (All dimensions in μm).

Component	**Single–"Hot" Arm Microactuator**						**Double–"Hot" Arm Microactuator**					
"Cold" Arm Length	150	200	250	300	350	400	150	200	250	300	350	400
"Cold" Arm Width	15	15	15	15	15	15	15	15	15	15	15	15
Flexure Length	62	62	62	62	62	62	62	62	62	62	62	62
Flexure Width	2	2	2	2	2	2	1.5	1.5	1.5	1.5	1.5	1.5
"Hot" Arm Length	212	262	312	362	412	462	212	262	312	362	412	462
"Hot" Arm Width	2	2	2	2	2	2	2.5	2.5	2.5	2.5	2.5	2.5
"Hot" and "Cold" Arm Separation	2	2	2	2	2	2	2	2	2	2	2	2
"Hot" Arm Separation	n/a	n/a	n/a	n/a	n/a	n/a	2	2	2	2	2	2

Table 2. Average Tip Deflection Force Delivered by the Single– and Double– "Hot" Arm Electrothermal Microactuators* to an Adjacent Simple Cantilever.

"Cold" Arm Length (μm)	**Single–"Hot" Arm Electrothermal Actuator Average Tip Force (μN)**	**Double–"Hot" Arm Electrothermal Actuator Average Tip Force (μN)**
150	3.2 (std. dev. = 0.086)	3.8 (std. dev. = 0.088)
200	4.7 (std. dev. = 0.093)	5.2 (std. dev. = 0.097)
250	8.1 (std. dev. = 0.104)	9.4 (std. dev. = 0.118)

* "Cold" arm lengths greater than or equal to 300 μm not included because the microactuator's motion was erratic and not reproducible.

the shuttle to change its position. Smooth continuous motion has been achieved by controlling the *relative* phase relationship between the set of independent square-wave voltage signals depicted in Fig. 5. When the *relative* phase relationship depicted in Fig. 5 is maintained, microengines incorporating single– and double–"hot" arm electrothermal actuators have been continuously operated under ambient conditions using square-wave frequencies spanning 0.1 Hz to 45 kHz for time periods exceeding 126 hours. Fig. 6 depicts the sequential motion of the pawl and translator required to move the shuttle. Fig. 7 depicts the translation of the shuttle depicted in Fig. 4 between the limits imposed by its internal slot and flange. Inertial loads (in the form of a geared mechanical translation shuttle), whose masses were more than 10 times that of the entire microengine, have been translated.

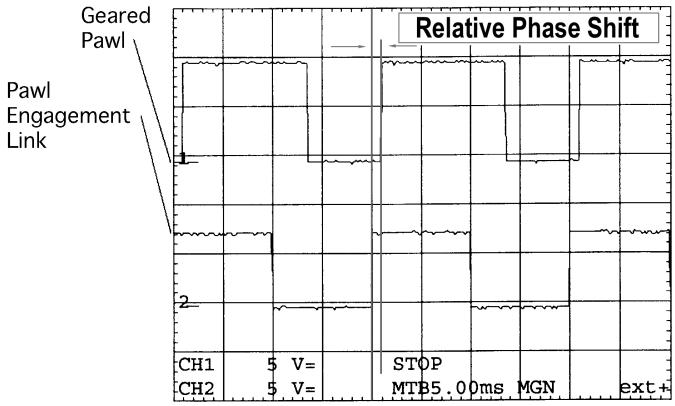

Fig. 5. Excitation waveform for the electrothermally-actuated microengine showing typical voltage amplitudes and the relative phase relationship for the two interdependent excitation signals.

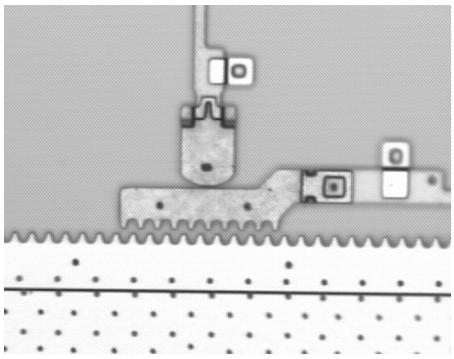

(a)

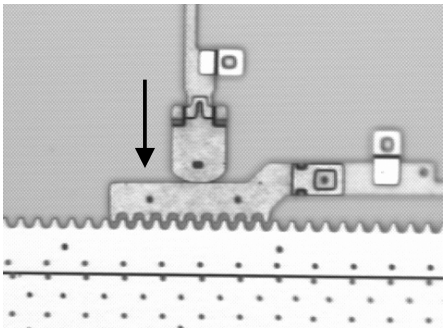

(b)

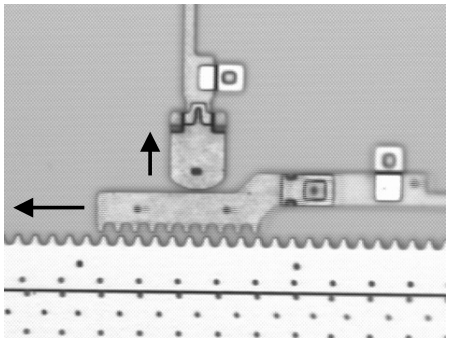

(c)

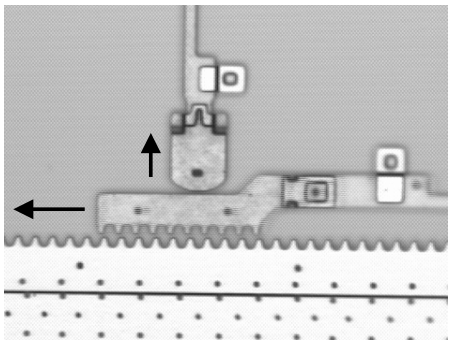

(d)

Fig. 6. Sequential motion of one pair of the pawl and translator elements depicted in Fig. 4 using the excitation waveform depicted in Fig. 5. (a) Equilibrium state. (b) Pawl engaging the translator. (c) Translator and engaged pawl moving the mechanical shuttle to the left. (d) Pawl disengaging from the translator just before it completes its motion to the left.

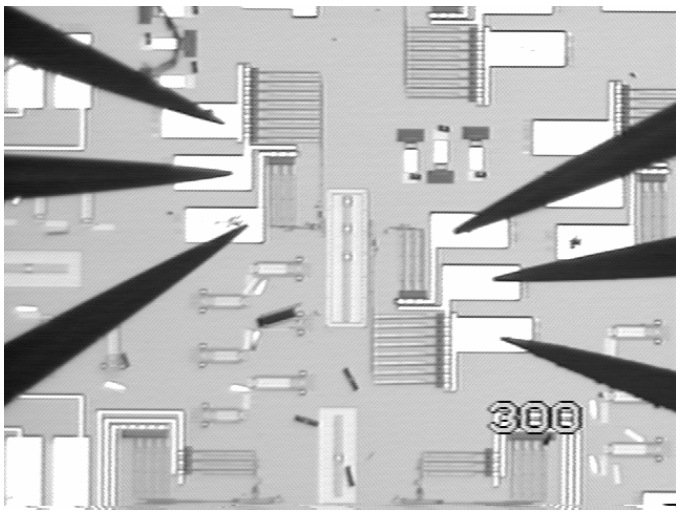

(a)

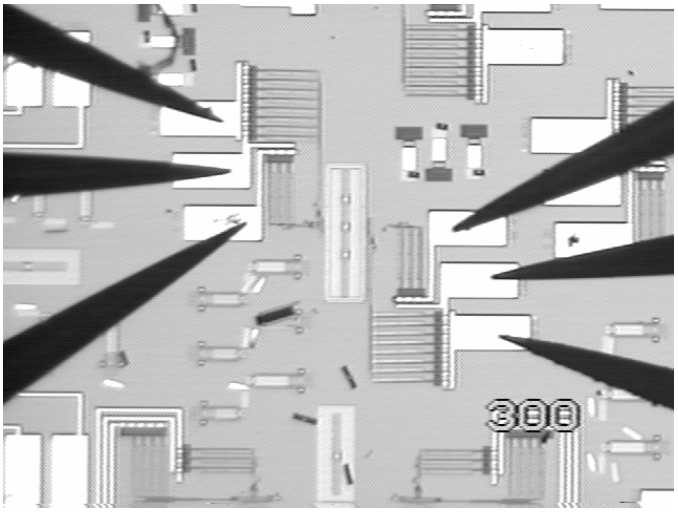

(b)

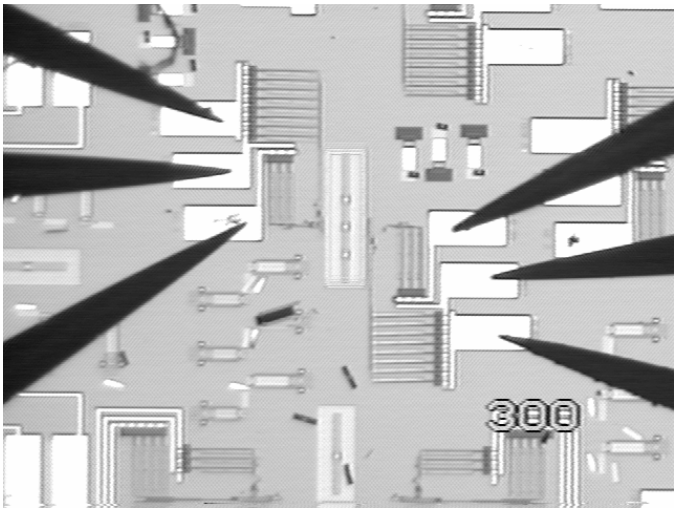

(c)

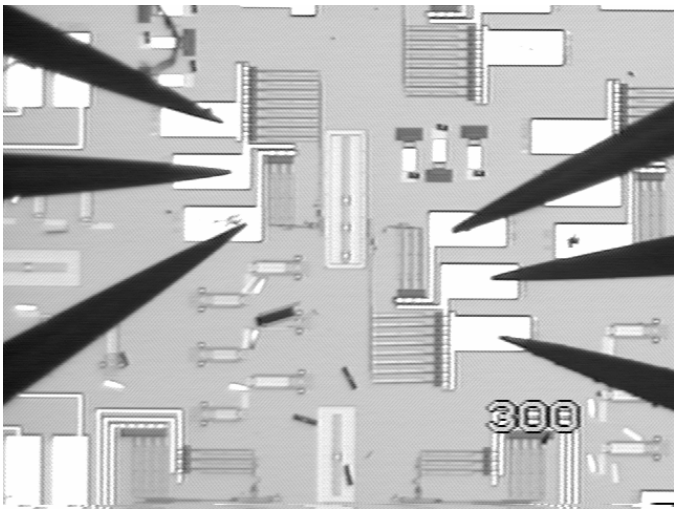

(d)

Fig. 7. Translation of the mechanical shuttle by the electrothermally-actuated microengine. The sequential action of the pawl and translator motion depicted in Fig. 6 was used to move the mechanical shuttle bi-directionally. The following sequence of four video captured frames depict the motion of the

mechanical shuttle as it moves from its lowest position to its up most position. (a) Mechanical shuttle in its lowest position. (b) Mechanical shuttle moving in an upward direction. (c) Mechanical shuttle poised to make contact with the lowest flange. (d) Mechanical shuttle translated to its uppermost position.

IV. Conclusion

Single– and double–"hot" arm electrothermal microactuators capable of producing in-plane tip deflections spanning 1–10 μm and generating tip forces exceeding 8 μN were designed and fabricated using the three-level polysilicon surface-micromachining foundry service that is available as the **M**ulti-**U**ser **M**icroelectromechanical Systems (MEMS) **P**roces**s** (MUMPS) through the JDS Uniphase Corporation. Microactuator tip deflections for both design variants were experimentally measured for devices whose "cold" arm length was 250 μm or less. For a given excitation power level, the double–"hot" arm electrothermal actuator produced an average 14 percent more tip deflection than a comparable single–"hot" arm device. The double–"hot" arm electrothermal microactuator with a 250 μm "cold" arm length generated approximately 16 percent more tip force compared to the single–"hot" arm device. Both electrothermal microactuator design variants with a "cold" arm length of 250 μm produced greater tip deflection magnitudes and generated greater tip forces compared to those devices with "cold" arm lengths of 150 μm and 200 μm. The electrothermal microactuators have been incorporated in an electrothermal microengine, and the position of a mechanical shuttle that can move bi-directionally has been controlled. The present research is focused on adapting this technology to function with a polymer lens and function similar to the network of ciliary muscles that focus the lens in the eye.

References

[1] L. Ristic, *Sensor Technology and Devices*, Norwood, MA: Artech House, 1994.

[2] C.S. Pan and W. Hsu, "An electro-thermally and laterally driven polysilicon microactuator," *J. Micromech. Microeng.*, vol. 7, pp. 7-13, 1997.

[3] H. Guckel, J. Klein, T. Cristenson, K. Skrobis, M. Laudon, and E.G. Lovell, "Thermo-magnetic metal flexure actuators," *in Tech. Dig. Solid-State Sen. Act. Workshop*, Hilton Head Island, SC, June 22-25, 1992, pp. 73-75.

[4] J.H. Comtois and V.M. Bright, "Surface micromachined polysilicon thermal actuator arrays and applications," in *Tech. Dig. Solid-State Sen. Act. Workshop*, Hilton Head Island, SC, June 2-6, 1996, pp. 174-176.

[5] G.K. Fedder and R.T. Howe, "Thermal assembly of polysilicon microstructures," *in Proc. IEEE Micro Electro Mechanical Systems Workshop*, Nara, Japan, January 30 – February 2, 1991, pp. 63-68.

[6] P.B. Allen, J.M. Wilken, and E.S. Kolesar, "Design, fabrication and performance evaluation of several electrical and mechanical silicon microstructures realized using the emerging technology of microelectromechanical systems (MEMS)," in *Proc. 1997 ASEE Conf.*, Houston, TX, March 23-25, 1997, pp. 43-48.

[7] D.N. Burns and V.M. Bright, "Design and performance of a double hot arm polysilicon thermal actuator," in *Proc. SPIE*, vol. 3224, October 1997, pp. 296-306.

[8] E.S. Kolesar, P.B. Allen, J.T. Howard, and J.M. Wilken, "Thermally actuated microbeam for large in-plane mechanical deflections," *J. Vac. Sci. Technol. A*, vol. 17, no. 4, July-August 1999, pp. 2257-2263.

[9] *L-Edit® CAD Software Manual*, version 7, Tanner Research, Inc., 180 North Vinedo Avenue, Pasadena, CA 91107.

[10] D. Koester, R. Mahedevan, A. Shishkoff, and K. Markus, *Multi-User MEMS Processes (MUMPS) Introduction and Design Rules*, revision 4, JDS Uniphase MEMS Technology Applications Center, 3021 Cornwallis Road, Research Triangle Park, NC 27709.

[11] I. Cochin and W. Cadwallender, *Analysis and Design of Dynamic Systems*, 3rd ed., Reading, MA: Addison-Wesley, 1997, pp. 309-353 and pp. 607-619.